Design and Implementation of Flight Dynamics Control Strategies for a Smartphone-based Quadrotor

Thesis for obtaining the degree of

Master of Science in Engineering
with emphasis in Automation

Alejandro Astudillo Vigoya
alejandro.astudillo@correounivalle.edu.co

School of Electrical and Electronic Engineering
UNIVERSIDAD DEL VALLE
Cali, COLOMBIA

November 7, 2017

Supervised by:

Dr.-Ing. Esteban Rosero
Industrial Control Research Group - GICI
School of Electrical and Electronic Engineering
Universidad del Valle

Bladimir Bacca Ph.D.
Perception and Intelligent Systems Research Group - PSI
School of Electrical and Electronic Engineering
Universidad del Valle

Abstract

The field of autonomous systems control is young, but operational experience is rapidly growing, making research on collaborative systems of great importance. Improving aerial robots in particular could be key in facing future environmental challenges..... In this work, two main problems are addressed: the cooperative source seeking problem and the cooperative level curve tracking problem by a group of agents under undirected constrained communications. ......

Contents

List of Figures

List of Tables

Chapter 1

Introduction

efwefwew

1.1 Motivation

wfwfew

1.2 Research Problem

wfewfe

1.3 Objectives

wefwefw

1.4 State of Art

wfwfewf

1.4.1 Quadrotors

wfwefwe

1.4.2 Smartphones as Controllers

wfwfwewf

1.4.3 Smartphone-based Quadrotors

wfwfwf

1.4.4 Quadrotor Flight Modes

wefwefewfw

Stabilize Mode

wfefef

Altitude Hold Mode

wefefwefwef

Loiter Mode

wfewfefwf

Return-To-Launch Mode

wfwefwefw

Auto Mode

wfwefwefwe

1.5 Outline

wefwefwefweffew

Chapter 2

Dynamic Model of the Quadrotor

tgrtnrttrr

2.1 Quadrotors' Configuration

rtbnrtbrtgtrgr

2.1.1 '+' Configuration

rtgrtgtrbrtgrg

2.1.2 'X' Configuration

rtgrtgrtgtrgrgr

2.2 Non-linear Model

This section describes the dynamic modeling used to perform the quadrotor control, based on the study carried out in Castillo and Lozano [2004], Tamami et al. [2014], Voos [2007]. This model represents the quadrotor as a solid symmetrical object subject to a total thrust and three torques, without considering the dynamics of the actuators.

The general coordinates representing the position and attitude of the quadrotor are defined as

$$q = \begin{bmatrix} \xi & \eta \end{bmatrix}^T , \tag{2.1}$$

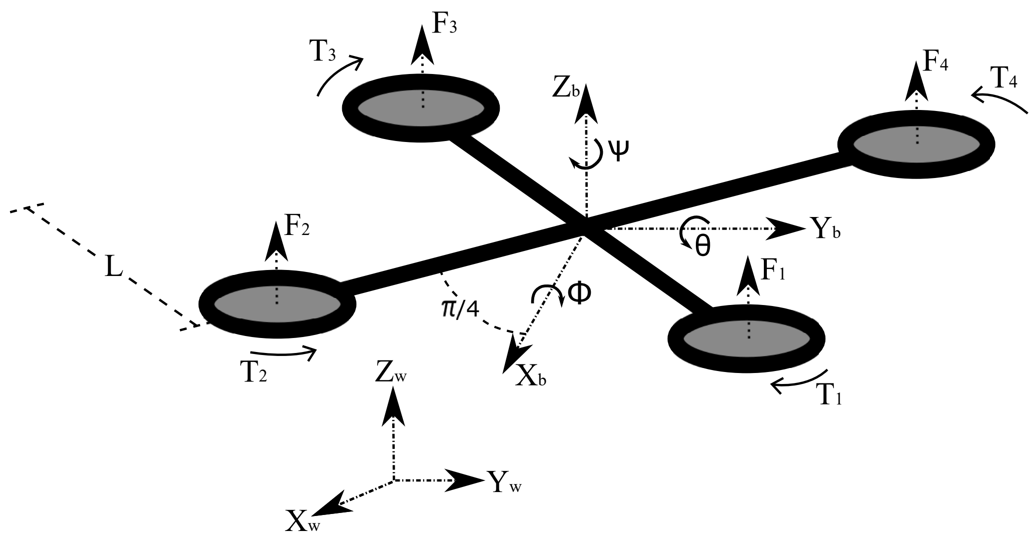

Figure 2.1: Quadrotor squeme with movement axis and thrust forces.

where $\xi = \begin{bmatrix} x & y & z \end{bmatrix}^T$ is the vector representing the position of the center of mass of the quadrotor relative to the body reference frame shown in Fig. 2.1 and $\eta = \begin{bmatrix} \psi & \theta & \phi \end{bmatrix}^T$ represent the quadrotor's attitude.

The Lagrangian of the quadrotor is defined by

$$L(q, \dot{q}) = K_{trans} + K_{rot} - U, \tag{2.2}$$

where $K_{trans} = \frac{m}{2}\dot{\xi}^T\dot{\xi}$ is the translational kinetic energy, $K_{rot} = \frac{1}{2}\dot{\eta}^T J\dot{\eta}$ is the rotational kinetic energy, $U = mgz$ is the potential energy, m is the quadrotor's mass , z is the quadrotor's elevation, g is the gravity acceleration magnitude, and J is the inertial matrix. The dynamic model of the quadrotor is derived from the Euler-Lagrange equation

$$\frac{d}{dt}\frac{\partial L}{\partial \dot{q}} - \frac{\partial L}{\partial q} = \begin{bmatrix} F_\xi \\ \tau \end{bmatrix}, \tag{2.3}$$

where $F_\xi = R_b^w \hat{F}_b$ is the translational force applied to the quadrotor by the four motors, τ contains the rolling, pitching and yawing torques, and

$$R_b^w = \begin{bmatrix} c\theta c\psi & c\psi s\theta s\phi - c\phi s\psi & s\phi s\psi + c\phi c\psi s\theta \\ c\theta s\psi & s\psi s\theta s\phi + c\phi c\psi & c\phi s\psi s\theta - s\phi c\psi \\ -s\theta & c\theta s\phi & c\theta c\phi \end{bmatrix} \tag{2.4}$$

is the rotation matrix from the body to the Earth frame where $c\theta = \cos\theta$ and $s\theta = \sin\theta$.

In the quadrotor's body frame, the translational force $\hat{F}_b$ is only applied in the z_b axis as shown in Fig. 2.1. This force is represented by

$$\hat{F}_b = \begin{pmatrix} 0 \\ 0 \\ u \end{pmatrix} = \begin{pmatrix} 0 \\ 0 \\ \sum_{i=1}^{4} F_i \end{pmatrix}, \tag{2.5}$$

with F_i being the force, in N, exerted by the motor M_i, as shown in Fig. 2.1.

The force F_i has a linear dependency with the square of the motor angular velocity, defined as

$$F_i = k_i w_i^2, \tag{2.6}$$

where w_i is the angular velocity of the motor, and k_i is a proportional constant. However, in practice F_i must be set using the PWM signal input of an ESC. The thrust-PWM relation is found experimentally and is shown in Section **??**.

The rolling, pitching and yawing torques contained in vector τ, are generated using the force exerted by each motor as

$$\tau = \begin{bmatrix} \tau_\psi \\ \tau_\theta \\ \tau_\phi \end{bmatrix} = \begin{bmatrix} T_1 + T_3 - T_2 - T_4 \\ Lcos(\pi/4)(F_3 + F_4 - F_2 - F_1) \\ Lcos(\pi/4)(F_2 + F_3 - F_1 - F_4) \end{bmatrix}, \tag{2.7}$$

where T_i is the torque produced by each motor along the z_b axis, L is the distance between each motor's rotor and the quadrotor's center of mass, and $Lcos(\pi/4)$ is the real distance between the point of application of the rolling and pitching torques and the quadrotor's center of mass along the x_b and y_b axes **?**.

The Euler-Lagrange equations can be divided in two parts, one for the ξ coordinates and another for the η coordinates, getting

$$\ddot{\xi} = \begin{bmatrix} \ddot{x} \\ \ddot{y} \\ \ddot{z} \end{bmatrix} = \begin{bmatrix} \frac{u_1}{m}(\cos\phi\sin\theta\cos\psi + \sin\phi\sin\psi) \\ \frac{u_1}{m}(\cos\phi\sin\theta\sin\psi - \sin\phi\cos\psi) \\ \frac{u_1}{m}(\cos\phi\cos\theta) - g \end{bmatrix}, \tag{2.8}$$

$$\ddot{\eta} = \begin{bmatrix} \ddot{\psi} \\ \ddot{\theta} \\ \ddot{\phi} \end{bmatrix} = \begin{bmatrix} \dot{\phi}\dot{\theta}\dfrac{J_{xx} - J_{yy}}{J_{zz}} + \dfrac{u_2}{J_{zz}} \\ \dot{\phi}\dot{\psi}\dfrac{J_{zz} - J_{xx}}{J_{yy}} + \dfrac{u_3}{J_{yy}} \\ \dot{\theta}\dot{\psi}\dfrac{J_{yy} - J_{zz}}{J_{xx}} + \dfrac{u_4}{J_{xx}} \end{bmatrix}, \tag{2.9}$$

where, $\begin{bmatrix} u_1, & u_2, & u_3, & u_4 \end{bmatrix}^T = \begin{bmatrix} u, & \tau_\psi, & \tau_\theta, & \tau_\phi \end{bmatrix}^T$, and (J_{xx}, J_{yy}, J_{zz}) are the moments of inertia around the quadrotor's body axes **??**.

The Euler-Lagrange equations in (2.8) and (2.9) are linearized using their Jacobian around the hover state where $\left[\eta,\ \dot{\eta},\ \dot{\xi}\right] \to \left[0,\ 0,\ 0\right]$, getting

$$\ddot{q} = \begin{bmatrix} g\theta \\ g\phi \\ u_1/m \\ u_2/J_{zz} \\ u_3/J_{yy} \\ u_4/J_{xx} \end{bmatrix}, \tag{2.10}$$

that is a simplified representation of the quadrotor complete model found in **?**.

2.3 Linearized Model

The linearized model of the quad-rotor helicopter written as a state space model is given by

$$\begin{aligned} \dot{x}(t) =& Ax(t) + Bu(t), \\ r(t) =& Cx(t), \end{aligned}$$

where

$$A = \begin{bmatrix} 0 & 1 & 0 & 0 & 0 & 0 & 0 & 0 & 0 & 0 & 0 & 0 \\ 0 & 0 & 0 & 0 & 0 & 0 & 0 & 0 & -g & 0 & 0 & 0 \\ 0 & 0 & 0 & 1 & 0 & 0 & 0 & 0 & 0 & 0 & 0 & 0 \\ 0 & 0 & 0 & 0 & 0 & 0 & 0 & 0 & 0 & 0 & g & 0 \\ 0 & 0 & 0 & 0 & 0 & 1 & 0 & 0 & 0 & 0 & 0 & 0 \\ 0 & 0 & 0 & 0 & 0 & 0 & 0 & 0 & 0 & 0 & 0 & 0 \\ 0 & 0 & 0 & 0 & 0 & 0 & 0 & 1 & 0 & 0 & 0 & 0 \\ 0 & 0 & 0 & 0 & 0 & 0 & 0 & 0 & 0 & 0 & 0 & 0 \\ 0 & 0 & 0 & 0 & 0 & 0 & 0 & 0 & 0 & 1 & 0 & 0 \\ 0 & 0 & 0 & 0 & 0 & 0 & 0 & 0 & 0 & 0 & 0 & 0 \\ 0 & 0 & 0 & 0 & 0 & 0 & 0 & 0 & 0 & 0 & 0 & 1 \\ 0 & 0 & 0 & 0 & 0 & 0 & 0 & 0 & 0 & 0 & 0 & 0 \end{bmatrix}$$

$$B = \begin{bmatrix} 0 & 0 & 0 & 0 & 0 & \frac{1}{m} & 0 & 0 & 0 & 0 & 0 & 0 \\ 0 & 0 & 0 & 0 & 0 & 0 & 0 & 1 & 0 & 0 & 0 & 0 \\ 0 & 0 & 0 & 0 & 0 & 0 & 0 & 0 & 0 & 1 & 0 & 0 \\ 0 & 0 & 0 & 0 & 0 & 0 & 0 & 0 & 0 & 0 & 0 & 1 \end{bmatrix}^T$$

$$C = \begin{bmatrix} 1 & 0 & 0 & 0 & 0 & 0 & 0 & 0 & 0 & 0 & 0 & 0 \\ 0 & 0 & 1 & 0 & 0 & 0 & 0 & 0 & 0 & 0 & 0 & 0 \\ 0 & 0 & 0 & 0 & 1 & 0 & 0 & 0 & 0 & 0 & 0 & 0 \end{bmatrix}^T$$

with the parameters

$m = 0.64$ kg,

$g = 9.81$ m/s.

The state vector is defined as

$$x(t) = \begin{bmatrix} r_x & \dot{r}_x & r_y & \dot{r}_y & r & \dot{r}_z \end{bmatrix}^T,$$

and the control inputs as

$$u(t) = \begin{bmatrix} u_1 & u_2 & u_3 & u_4 \end{bmatrix}^T,$$

and the output vector is defined as

$$r(t) = \begin{bmatrix} r_x & r_y & r_z \end{bmatrix}^T.$$

2.4 Conclusions

aaaa

Chapter 3

Smartphone-based Quadrotor Prototype

qwqw

3.1 Description of the Components

qwqwq

3.1.1 Smartphone

qwqwq

3.1.2 Frame

qwqwq

3.1.3 Motors and Electronic Speed Controllers (ESC)

qwqwqw

3.1.4 Smartphone-ESC Gateway

qwqwqwq

3.1.5 Battery

qwqwqw

3.1.6 Assembled Smartphone-based Quadrotor

qwqwq

3.2 Quadrotor Parameters

qwqwqw

3.2.1 Mass

qwqw

3.2.2 Inertial Momentum

qwqwqw

3.2.3 Motors Thrust

qwqwqwqw

3.2.4 Motors Torque

qwqwqwq

3.3 Conclusions

qwqwqwqw

Chapter 4

Control Strategies and State Estimation

rtrtrtrtr

4.1 Control Strategies

ghgfhhff

4.1.1 Linear Quadratic Regulator

hhfhfhg

4.1.2 H_∞ Controller

fhfhfhfgfh

4.2 Controllers Design

fhfgfhfh

4.2.1 Stabilize Mode

fghgfh

Dynamic Model

rtrterere

Linear Quadratic Regulator

rtrterere

H_∞ Controller

rtrtererre

4.2.2 Altitude Hold Mode

Dynamic Model

rtrterere

Linear Quadratic Regulator

rtrterere

H_∞ Controller

rtrtererre

4.2.3 Loiter Mode

Dynamic Model

rtrterere

Linear Quadratic Regulator

rtrterere

H_∞ Controller

rtrtererre

4.2.4 Return-To-Launch Mode

Dynamic Model

rtrterere

Linear Quadratic Regulator

rtrterere

H_∞ Controller

rtrtererre

4.2.5 Auto Mode

Dynamic Model

rtrterere

Linear Quadratic Regulator

rtrterere

H_∞ Controller

rtrtererre

4.3 State Estimation Through Kalman Filter

tytytyty

4.3.1 Particle Model

rtrtrtrtrt

4.3.2 Quadrotor Model

ytytyttytt

4.4 Conclusions

rtrtrrtrtr

Chapter 5

Implementation and Results

rgrtgrtgrgtrgrrg

5.1 Kalman Filter for State Estimation

rtgrtgtrgtr

5.2 Linear Quadratic Regulator Results

grtgrgtrgtrgtrg

5.2.1 Simple Translational Movements (LQR)

grtgtrgrtgrg

5.2.2 Trajectory Tracking (LQR)

trgrgrtgtrgr

5.3 H∞ Regulator Results

grgtrgrgtrg

5.3.1 Simple Translational Movements ($H\infty$)

grtgrgrtgrtgtrg

5.3.2 Trajectory Tracking ($H\infty$)

rgrtgrtgrgtrgrg

5.4 Conclusions

rgrgrgtrgrtgr

Conclusions and Outlook

In this thesis distributed algorithms

Publications

A. Astudillo, P. Muñoz, F. Alvarez and E. Rosero, "Altitude and attitude cascade controller for a smartphone-based quadcopter," in *2017 International Conference on Unmanned Aircraft Systems (ICUAS)*. IEEE, jun 2017, pp. 1447–1454. [Online]. Available: http://ieeexplore.ieee.org/document/7991400/

A. Astudillo, B. Bacca and E. Rosero, "Optimal and robust controllers design for a smartphone-based quadrotor," in *2017 IEEE 3rd Colombian Conference on Automatic Control (CCAC)*

(Paper Submitted to Journal) A. Astudillo, P. Muñoz and E. Rosero, "Cascade Controller for Autonomous Flight of a Smartphone-based Quadrotor," in *Journal of Intelligent & Robotic Systems, SI: UAS-2017.*

Supplementary Material

Video of experiments: https://goo.gl/vQ3sZx

Bibliography

P. Castillo and R. Lozano. Stabilization of a mini-rotorcraft having four rotors, 2004.

N. Tamami, E. Pitowarno, and I. Astawa. Proportional derivative active force control for “x” configuration quadcopter, 2014.

H. Voos. Nonlinear control of a quadrotor micro-uav using feedback-linearization, 2007.